J. Sep. Sci. 2001, *24*, 87–96

Glenn S. Frysinger, Richard B. Gaines

U.S. Coast Guard Academy, Department of Science, 27 Mohegan Avenue, New London, CT 06320-8101, USA

Separation and identification of petroleum biomarkers by comprehensive two-dimensional gas chromatography

Comprehensive two-dimensional gas chromatography (GC × GC) has been used to separate and identify biomarker molecules in crude oil. The biomarkers examined include alkylated aromatics (naphthalenes, biphenyls, fluorenes, phenanthrenes, chrysenes), sulfur-containing aromatics (dibenzothiophenes, benzonaphthothiophenes), steranes, triterpanes, and triaromatic steranes. These biomarkers, which are frequently used in forensic oil spill analysis and petroleum exploration, were separated into easily recognizable bands in the GC × GC chromatogram. Methods used to identify the bands included peak matching with chemical standards, comparison with GC/MS extracted ion chromatograms, and the application of chemical logic based on the known volatility and polarity properties of the biomarkers.

Key Words: GC × GC; Comprehensive two-dimensional gas chromatography; Crude oil; Petroleum; Biomarkers; Steranes; Triterpanes; Hopanes

Ms received: June 23, 2000; accepted: December 21, 2000

1 Introduction

Crude oil contains numerous "chemical fossil" or "biomarker" molecules, which are resistant to degradation, and whose origin in the crude oil is related through transformation to organic molecules produced by living organisms [1, 2]. Biomarker molecules are widely used by petroleum geochemists in oil exploration because they can relate crude oil to its source and indicate oil maturity [3]. Biomarkers are also used by analytical chemists to trace spilled, weathered, and biodegraded petroleum pollution in the environment [4, 5].

The two best-known and abundant biomarkers in petroleum are the isoprenoid molecules, pristane and phytane. The isoprenoid biomarkers are derived from chlorophyll degradation as well as from direct bacterial input [1]. Other less abundant biomarkers in petroleum are the steranes and triterpanes. The sterane biomarkers are derived from sterols that are found in higher plants and algae. Sterane biomarkers have a tetracyclic structure and an alkyl side-chain. The numerous members of the sterane class vary primarily in the configuration of the alkyl side-chain, but some also vary in the position of methyl group substitution on the rings. In addition, steranes exhibit stereochemistry due to chiral carbon atoms at the ring junctions [6]. The triterpane biomarkers are derived from triterpenoids found in bacteria [2, 6]. Triterpanes may be tricyclic, tetracyclic, or pentacyclic. The most geochemically important group are the pentacyclic hopanes [6]. Other important biomarkers in petroleum are the alkylated naphthalene, phenanthrene, and chrysene aromatics, and the dibenzothiophene and benzonaphthothiophene sulfur-containing aromatics. These aromatic components are also considered biomarkers because, like the isoprenoids, steranes, and hopanes, they are persistent chemical markers in the petroleum.

Separation and identification of petroleum biomarkers are challenging because the biomarkers are often minor components of an extremely complex mixture. High resolution gas chromatographic separations of crude oil produce a chromatogram that typically has only 100 peaks lying on a baseline hump of unresolved components. At any point in the chromatogram, there are likely more than ten components contributing to the unresolved complex mixture hump, therefore gas chromatography alone is not suitable for analysis of minor biomarker components.

Hyphenated techniques, such as gas chromatography coupled with mass spectrometry (GC/MS) can provide a more complete separation and identification. The chromatography partially separates the complex mixture and the mass spectrometer acts as a second separation or chemical structure identification mechanism. In GC/MS analysis, the extracted ion chromatogram (EIC) is used to isolate a specific class of petroleum biomarker molecules. In

Correspondence: Prof. Glenn S. Frysinger, U.S. Coast Guard Academy, Department of Science, 27 Mohegan Avenue, New London, CT 06320-8101, USA.
E-mail: gfrysinger@cga.uscg.mil
Fax: +1 860 701 6147

1615-9306/2001/0202–0087$17.50+.50/0

some cases, the EIC for the molecular ion mass is used to identify the biomarkers. For example, the *m/z* 156 EIC contains peaks showing the distribution of two-carbon substituted naphthalene isomers present in the crude oil. In other cases, the EIC of a significant fragment ion is used. For example, the many different sterane biomarkers have a common *m/z* 217 fragment in their mass spectrum so they are observed using the *m/z* 217 EIC [2, 5]. However, the EIC for a specific class can contain extra peaks if unrelated molecules produce the same mass fragment. One solution commonly used to improve the separation and identification of specific biomarkers is GC/MSMS analysis. In MSMS detection, soft ionization of the molecules allows molecular ion separation before hard ionization, fragment separation, and mass spectrum generation [3, 6].

Comprehensive two-dimensional gas chromatography (GC × GC) is a hyphenated technique where two different chromatographic separation mechanisms act in concert to greatly improve component separation and identification [7, 8]. To date, GC × GC has been used primarily to analyze light and middle distillate petroleum products. GC × GC has successfully separated and quantitated oxygenates [9], and benzene, toluene, ethylbenzene, xylenes (BTEX), and heavier aromatics in gasoline [10]. GC × GC has been used to study the composition of kerosene [11], gas oil [12], cycle oil [13], and for forensic fingerprinting of a marine diesel fuel spill [14]. GC × GC has also been interfaced to a mass spectrometer to identify peaks in GC × GC chromatograms of petroleum fuels [15, 16]. In this work, GC × GC has been applied to the analysis of crude oil, with particular attention to the separation and identification of biomarkers used in forensic oil spill analysis and petroleum exploration.

2 Materials and methods

2.1 GC × GC system

The GC × GC system consists of an HP 6890 gas chromatograph (Hewlett-Packard, Wilmington, DE, USA) containing two chromatography columns with different selectivity, a thermal modulator assembly (Zoex Corp, Lincoln, NE, USA), and a flame ionization detector.

The thermal modulator is used to transfer analyte between the two chromatographic dimensions in GC × GC [17]. The main elements of the thermal modulator are a small section of capillary column called the "modulator tube" and a rotating slotted heater. The modulator tube is a short, 8-cm-section of capillary column that provides significant analyte retention, typically with a retention factor greater than 40. The slotted heater, with a temperature 100°C greater than the modulator tube temperature, periodically rotates over the modulator tube to desorb the analyte, focus it, and inject it into the second column. The half-height width of the injected band is less than 100 ms. The modulator repeats the injection every 5 s.

In the present experiment, a nonpolar dimethylpolysiloxane stationary phase provided volatility-based selectivity in the first dimension. A 50% phenyl polysiphenylene-siloxane phase provided polarity-based selectivity in the second dimension. This phase combination was effective for separating petroleum components. The first dimension used a $2^{\circ}\ min^{-1}$ temperature program to produce carbon number separation in 140 min. During that time period, nearly 1700 fast 5-s isothermal separations were completed on the second dimension to separate the chemical classes.

The first column, modulator tube, and second column were temperature controlled and programmed independently. The main advantage of independent temperature control is that the modulator tube capillary can be held at a lower temperature than the first column to increase retention and eliminate analyte breakthrough between modulator cycles. In this experiment, a 40°C cooler temperature provided sufficient retention and trapping on a thin-film (0.5 μm) modulator tube capillary. Since thin-film capillaries have a higher temperature limit, the range of GC × GC analysis was extended to C_{40} alkanes. The 8-cm modulator tube capillary was connected to two sections of deactivated transfer line with small, glass press-fit connectors. As a result, the entire length of the 8-cm modulator tube is heated and desorbed by the rotating heater. Independent temperature control of the second column allows temperature tuning of the component retention factor on the second column for fast GC separations.

Specific GC × GC operating conditions are listed in **Table 1.**

2.2 GC/MS system

The GC/MS system is an HP GCD Plus (Hewlett-Packard, Wilmington, DE, USA). The system integrates an HP 5890 GC oven with an HP 5972-series quadrupole mass spectrometer. In the experiment, the GC/MS was operated in a full scan mode. Several chromatograms were obtained with reduced mass range (150–235 and 230–450) to increase ion dwell time and improve signal to noise. Extracted ion chromatograms (EICs) were prepared for comparison with the GC × GC data.

The GC/MS system used a column identical to the first dimension of the GC × GC system. However, to closely match resolution performance and retention times of the GC × GC system, a long detector transfer line was added to minimize the vacuum pressure drop in the column. GC × GC first-dimension retention times were reproduced on the GC/MS to within 3%. GC × GC and GC/MS chro-

Table 1. GC × GC chromatographic conditions.

Columns	Injector transfer line	0.40 m × 0.100 mm deactivated column
	1st column	10.00 m × 0.100 mm × 0.5 μm dimethylpolysiloxane (Phase 007-1, Quadrex, New Haven, CT, USA)
	1st column temperature	50–320°C @ 2° min^{-1} (40 min)
	Modulator tube	0.15 m × 0.100 mm deactivated column
		0.08 m × 0.100 mm × 0.5 μm dimethylpolysiloxane
		0.15 m × 0.100 mm deactivated column
	Modulator tube temperature	40 (15 min) – 300°C @ 2° min^{-1} (30 min)
	2nd column	0.50 m × 0.100 mm × 0.10 μm 50% phenyl polysiphenylenesiloxane (Phase BPX-50, SGE, Austin, TX, USA)
	2nd column temperature	80–360°C @ 2° min^{-1} (35 min)
	Detector transfer line	0.25 m × 0.100 mm deactivated column
Injection	200 mg mL^{-1} crude oil in CH_2Cl_2, 2.0 μL, 20/1 split, 300°C	
Detection	FID 375°C	
Flow	H_2, 0.4 mL min^{-1} constant flow 25.7–48.7 psi @ 0.177 psi min^{-1}	
Modulator	ΔT=100°C velocity, 0.25 rev s^{-1}, period 5.0 s	

Table 2. GC/MS chromatographic conditions.

Columns	Injector transfer line	0.5 m × 0.100 mm deactivated column
	Column	10.0 m × 0.100 mm × 0.5 μm dimethylpolysiloxane (Phase 007-1, Quadrex, New Haven, CT, USA)
	Column temperature	40–300°C @ 2° min^{-1}
	Detector transfer line	3.7 m × 0.100 mm deactivated column
Injection	200 mg mL^{-1} crude oil in CH_2Cl_2, 2.0 μL, 10/1 split, 300°C	
Flow	H_2, 0.4 mL min^{-1} constant flow 27.1–53.9 psi @ 0.206 psi min^{-1}	

matograms were aligned by linearly scaling the GC/MS EIC *n*-alkane interval to match the corresponding *n*-alkane interval in the GC × GC chromatogram.

Specific operating conditions are listed in **Table 2**.

2.3 Crude Oil Sample

The crude oil analyzed in this study is *Exxon Valdez* cargo oil, which was sampled by the United States Coast Guard on April 2, 1988. The chemical composition of this crude oil has been extensively studied [4, 18–20].

3 Results and Discussion

The GC × GC chromatogram of crude oil is shown in **Figure 1**. The first dimension of the GC × GC separation has volatility-based selectivity to separate the petroleum components by carbon number. The major peaks distributed from left to right across the *x*-axis of the GC × GC chromatogram are the C_{10} to C_{38} *n*-alkanes. The second dimension has polarity-based selectivity to separate components by chemical class. Peaks separated from bottom to top on the *y*-axis are the alkanes, single- and multi-ring cycloalkanes, and one-, two-, three-, and four-ring aromatics. In this manner, GC × GC is effective at separating, grouping, and identifying the important classes of petroleum biomarkers in a complex crude oil sample. Several types of biomarker compounds are highlighted in boxes on the GC × GC chromatogram. The peak identities and patterns of these selected biomarker components are analyzed in Figure 2 to Figure 5. The GC × GC chromatogram patterns were decoded with a combination of chemical standards, direct comparison with GC/MS EICs, and the application of chemical logic given the known volatility and polarity properties of the biomarkers.

An extracted region of the complete GC × GC chromatogram of crude oil is shown in **Figure 2**. The prominent group of peaks at the left of the GC × GC chromatogram between 40 and 45 min on the first dimension and about 1.5 to 2.0 s retention on the second-dimension are the two-carbon substituted naphthalenes (C_2N). The GC/MS *m/z* 156 EIC is aligned with the GC × GC peaks and shows excellent retention and mass abundance corre-

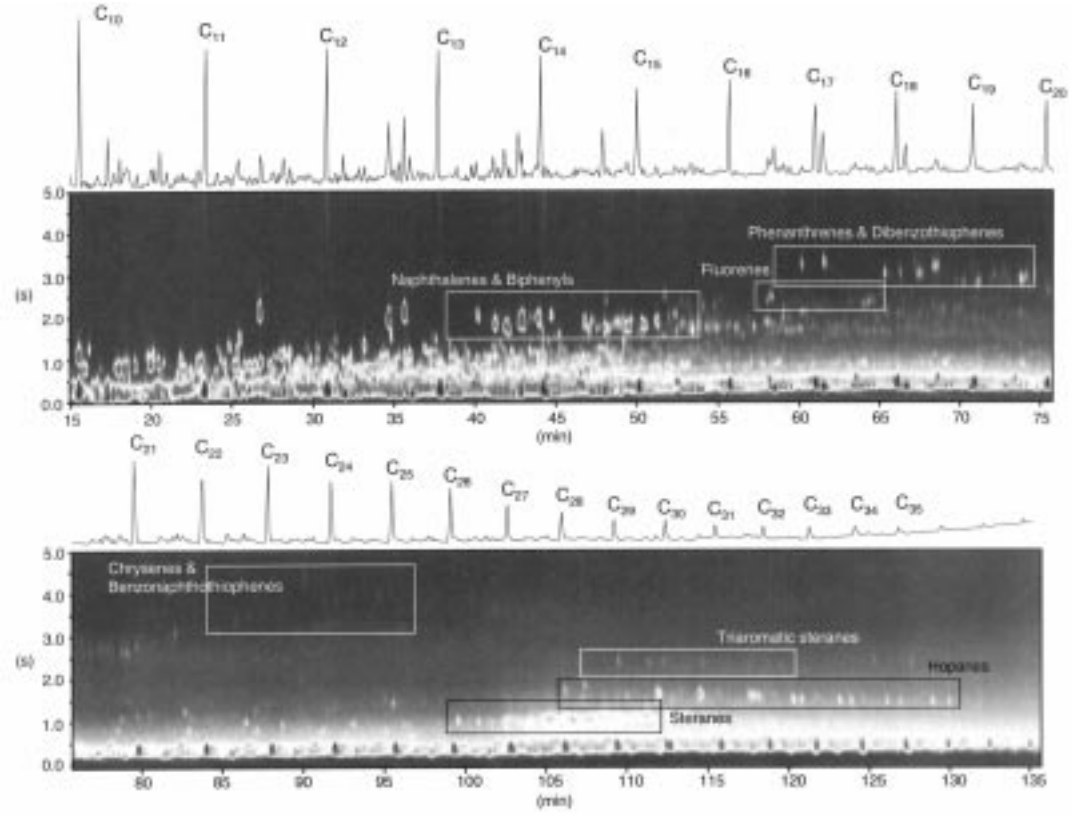

Figure 1. GC × GC chromatogram of crude oil. The *x*-axis is the first dimension volatility-based separation (minutes). The *y*-axis is the second dimension polarity-based separation (seconds). The *z*-axis is FID response; to improve color contour visualization, $\log_{10}$FID response is displayed to compress the large dynamic range between the most and least abundant peaks. Groups of significant biomarker compounds are identified in boxes. The corresponding one-dimensional volatility-based gas chromatogram is overlaid for comparison.

spondence. The identity of some peaks in the *m/z* 156 EIC are known by comparison with published GC/MS EIC patterns. Peaks numbered on the EICs in Figure 2 are identified in **Table 3**.

One difference observed between the *m/z* 156 EIC and the GC × GC pattern is resolution. Some peaks that are nearly resolved in the EIC are not resolved in the GC × GC chromatogram. This reduction in resolution results from the discrete sampling performed with the thermal modulator, which reduces the effective first dimension data sampling rate to 0.2 Hz. Differences may also be observed in the mass abundance. The GC × GC peaks represent the total mass of each component in the crude oil sample while the EICs reflect the abundance of the molecular ion. One other peak near the beginning of the C_2N band in the GC × GC chromatogram was identified as biphenyl (BP) using chemical standards. Two-carbon substituted naphthalenes and biphenyl logically appear near each other in the GC × GC chromatogram because each has 12 carbon atoms and 2 aromatic rings. These chemical similarities yield similar volatility and polarity-based retention in the two dimensions of the GC × GC separation.

The *m/z* 170 EIC for three-carbon substituted naphthalenes (C_3N) also corresponds to a group of peaks in the GC × GC chromatogram. However, there are peaks found early in the GC × GC band that are not in the *m/z* 170 EIC. Further investigation revealed that those GC × GC peaks correspond to the pattern of peaks in the *m/z* 168 EIC. Therefore, those GC × GC peaks include isomers of one-carbon substituted biphenyls (C_1BP). Using the same chemical logic as above, it is expected that C_3N and C_1BP groups will appear at the same volatility and polarity position in the GC × GC chromatogram since both groups have 13 carbon atoms, and 2 aromatic rings. One other peak identified in the GC × GC chromatogram is fluorene (FL). Note that it is found at greater second-dimension retention than the naphthalenes and biphenyls. Fluorene has two aromatic rings plus a five-membered ring. The additional ring contributes to the overall polarity of the molecule and therefore produces more retention on the polar second-dimension column.

Table 3. Extracted ion chromatogram peak identities for Figure 2 – Figure 5.

Peak no.	Peak Identity	Reference
1	2,6-dimethylnaphthalene	[21]
2	2,7-dimethylnaphthalene	[21]
3	1,3-dimethylnaphthalene, 1,7-dimethylnaphthalene	[21]
4	1,6-dimethylnaphthalene	[21]
5	1,5-dimethylnaphthalene	[21]
6	1,2-dimethylnaphthalene	[21]
7	1,3,7-trimethylnaphthalene	[21, 22]
8	1,3,8-trimethylnaphthalene	[21, 22]
9	1,4,6-trimethylnaphthalene, 1,3,5-trimethylnaphthalene	[21, 22]
10	2,3,6-trimethylnaphthalene	[21, 22]
11	1,2,4-trimethylnaphthalene	[21]
12	1,2,5-trimethylnaphthalene	[21, 22]
13	3-methylbiphenyl	[23]
14	4-methylbiphenyl	[23]
15	4-methyldibenzothiophene	[21, 24–26]
16	2-methyldibenzothiophene, 3-methyldibenzothiophene	[21, 24–26]
17	1-methyldibenzothiophene	[21, 24–26]
18	4-ethyldibenzothiophene	[21]
19	4,6-dimethyldibenzothiophene	[21]
20	2,4-dimethyldibenzothiophene	[21]
21	2,6-dimethyldibenzothiophene, 3,6-dimethyldibenzothiophene	[21]
22	1,4-dimethyldibenzothiophene	[21]
23	1,3-dimethyldibenzothiophene	[27]
24	2-methylfluorene	[28]
25	1-methylfluorene	[28]
26	3-methylphenanthrene	[29, 21]
27	2-methylphenanthrene	[29, 21]
28	9-methylphenanthrene, 4-methylphenanthrene	[29, 21]
29	1-methylphenanthrene	[29, 21]
30	3,6-dimethylphenanthrene, 2- ethylphenanthrene, 3-ethylphenanthrene	[29, 21]
31	1-ethylphenanthrene	[29, 21]
32	2,6-dimethylphenanthrene, 3,5-dimethylphenanthrene	[29, 21]
33	2,7-dimethylphenanthrene	[29, 21]
34	3,10-dimethylphenanthrene, 1,3-dimethylphenanthrene, 2,10-dimethylphenanthrene, 3,9-dimethylphenanthrene	[29, 21]
35	1,6-dimethylphenanthrene, 2,5-dimethylphenanthrene, 2,9-dimethylphenanthrene	[29, 21]
36	1,7-dimethylphenanthrene	[29, 21]
37	2,3-dimethylphenanthrene	[29, 21]
38	1,9-dimethylphenanthrene, 4,9-dimethylphenanthrene, 4,10-dimethylphenanthrene	[29, 21]
39	1-methyl benzo[*b*]naphtho[2,1-*d*]thiophene	[27]
40	5α,13β,17α(*H*)-diacholestane (20*S*)	[2, 30, 32]
41	5α,13β,17α(*H*)-diacholestane (20*R*)	[30, 32]
42	5α,13α,17β(*H*)-diacholestane (20*S*)	[30, 32]
43	24-methyl-5α,13α,17β(*H*)-diacholestane (20*R*), 5α,14α,17α(*H*)-cholestane (20*S*)	[30]
44	24-ethyl-5α,13β,17α(*H*)-diacholestane (20*S*)	[30, 33]
45	5α,14β,17β(*H*)-cholestane (20*R*)	[30]
45	5α,14β,17β(*H*)-cholestane (20*S*)	[30]
46	5α,14α,17α(*H*)-cholestane (20*R*)	[30]
47	24-ethyl-5α,13β,17α(*H*)-diacholestane (20*R*)	[30]
48	24-methyl-5α,14β,17β(*H*)-cholestane (20*R*) 24-ethyl-5α,13α,17β(*H*)-diacholestane (20*R*)	[30, 31]
49	24-methyl-5α,14β,17β(*H*)-cholestane (20*S*)	[30, 31]
50	24-methyl-5α,14α,17α(*H*)-cholestane (20*R*)	[19, 30, 31]
51	24-ethyl-5α,14α,17α(*H*)-cholestane (20*S*)	[19, 30, 31]
52	24-ethyl-5α,14β,17β(*H*)-cholestane (20*R*)	[30, 31]
53	24-ethyl-5α,14β,17β(*H*)-cholestane (20*S*)	[30, 31]
54	24-ethyl-5α,14α,17α(*H*)-cholestane (20*R*)	[2, 19, 30, 31]
55	18α(*H*)-22,29,30-trisnorneohopane	[3, 6, 30, 32]

Table 3. Continued.

Peak no.	Peak Identity	Reference
56	17α(*H*)-22,29,30-trisnorhopane	[3, 6, 30, 32]
57	17α,21β(*H*)-30-norhopane	[3, 6, 30, 32]
58	17α,21β(*H*)-hopane	[3, 6, 30, 32]
59	17α,21β(*H*)-homohopane (22*S*)	[3, 6, 30, 32]
60	17α,21β(*H*)-homohopane (22*R*)	[3, 6, 30, 32]
61	17α,21β(*H*)-bishomohopane (22*S*)	[3, 6, 30, 32]
62	17α,21β(*H*)-bishomohopane (22*R*)	[3, 6, 30, 32]
63	17α,21β(*H*)-trishomohopane (22*S*)	[3, 6, 30, 32]
64	17α,21β(*H*)-trishomohopane (22*R*)	[3, 6, 30, 32]
65	17α,21β(*H*)-tetrakishomohopane (22*S*)	[3, 6, 30, 32]
66	17α,21β(*H*)-tetrakishomohopane (22*R*)	[3, 6, 30, 32]
67	17α,21β(*H*)-pentakishomohopane (22*S*)	[3, 6, 30, 32]
68	17α,21β(*H*)-pentakishomohopane (22*R*)	[3, 6, 30, 32]
69	cholestane (20*S*)	[3, 29, 34]
70	cholestane (20*R*) + 24-methylcholestane (20*S*)	[3, 29, 34]
71	24-ethylcholestane (20*S*)	[3, 29, 34]
72	24-methylcholestane (20*R*)	[3, 29, 34]
73	24-ethylcholestane (20*R*)	[3, 29, 34]

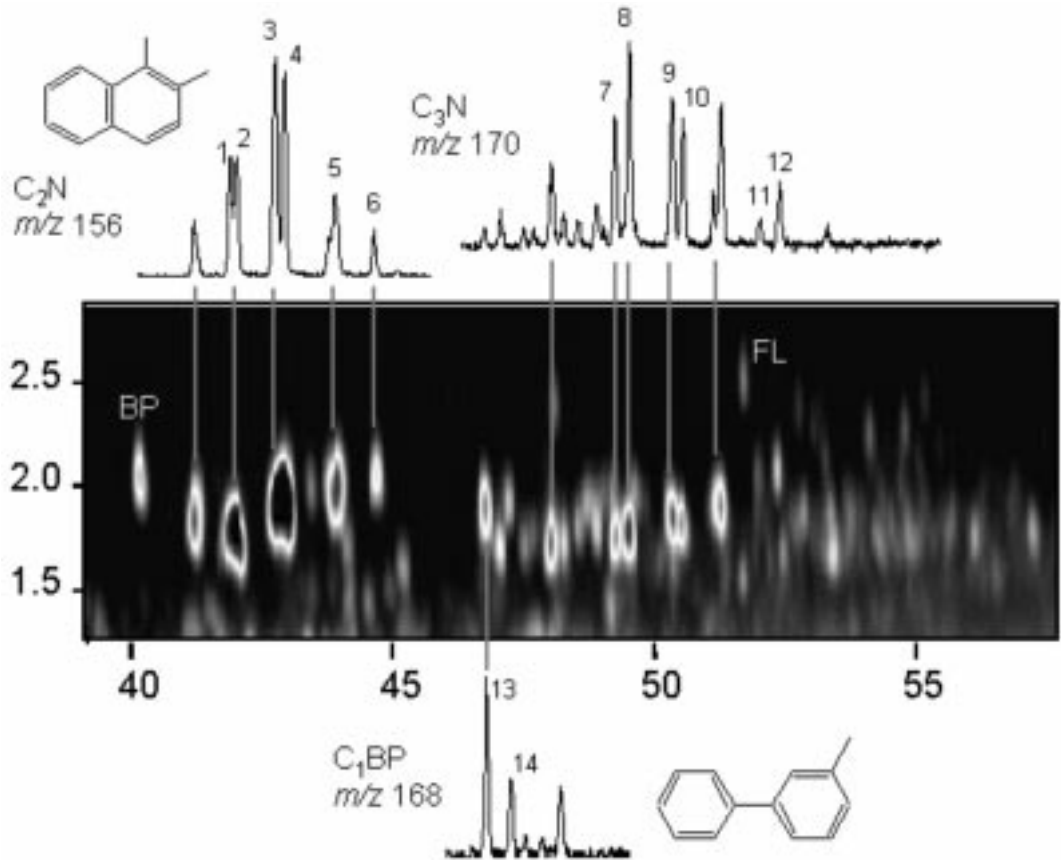

Figure 2. Extracted region of the GC × GC chromatogram. Biphenyl (BP) and fluorene (FL) peaks are identified. GC/MS extracted ion chromatograms (EIC) of substituted biphenyls (C_xBP) and naphthalenes (C_xN) are overlaid for identification and comparison. Connecting lines are drawn for the major peaks to show the correspondence between the GC/MS and GC × GC data. Peaks numbered on each EIC are identified in Table 3. The structures of 1,2-dimethylnaphthalene (peak 6) and 3-methylbiphenyl (peak 13) are included for reference.

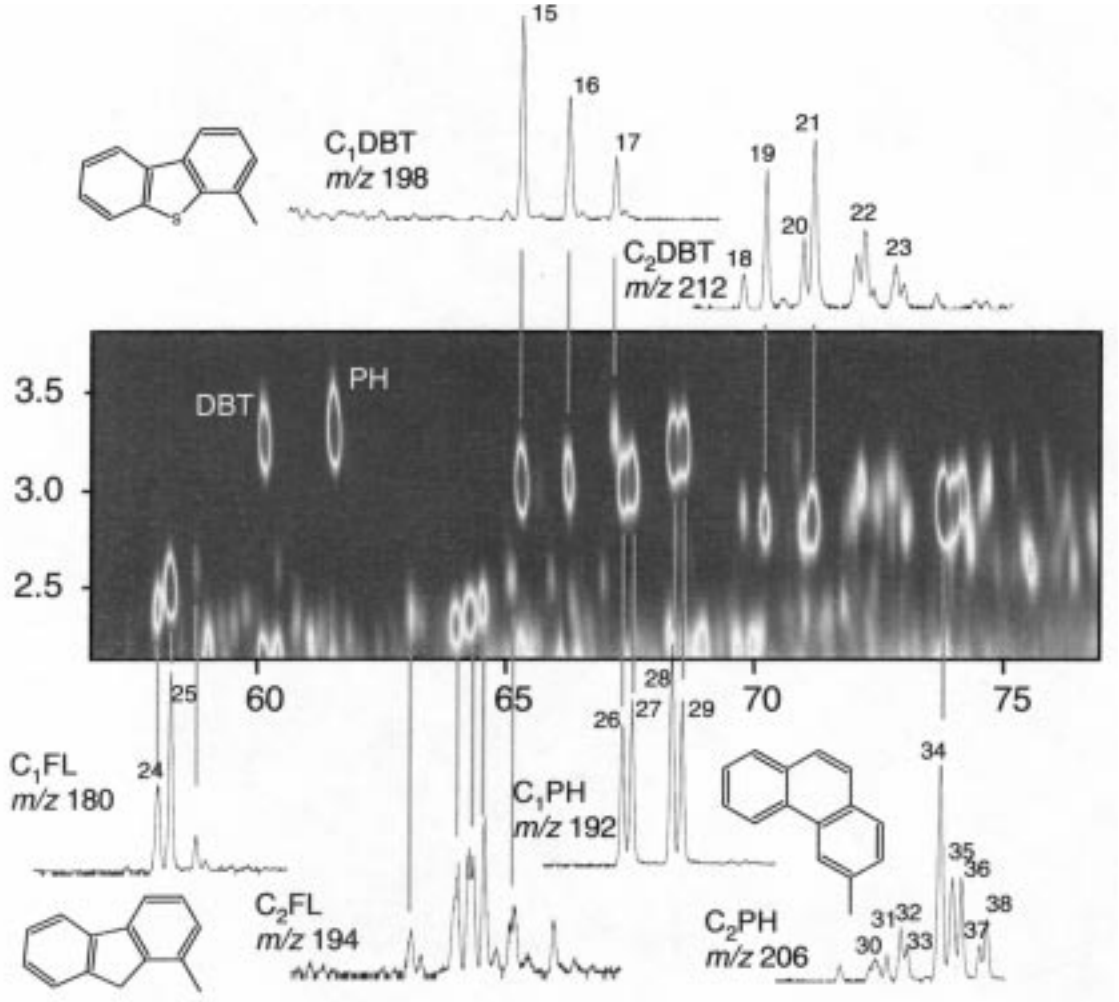

Figure 3. Extracted region of the GC × GC chromatogram. Dibenzothiophene (DBT) and phenanthrene (PH) peaks are identified. GC/MS extracted ion chromatograms (EIC) of substituted fluorenes (C_xFL), dibenzothiophenes (C_xDBT), and phenanthrenes (C_xPH) are overlaid for identification and comparison. Peaks numbered on each EIC are identified in Table 3. The structures of 4-methyldibenzothiophene (peak 15), 1-methylfluorene (peak 25), and 3-methylphenanthrene (peak 27) are included for reference.

A GC × GC chromatogram region containing carbon substituted fluorenes (C_1FL, C_2FL), substituted phenanthrenes (C_1PH, C_2PH), and substituted dibenzothiophenes (C_1DBT, C_2DBT) is shown in **Figure 3**. The one- and two-carbon substituted fluorene bands range from about 55 to 67 min on the first dimension and about 2.5 s on the second dimension. The substituted fluorenes are found at approximately the same second-dimension retention time as the unsubstituted fluorene in Figure 2. These fluorene bands correspond to the *m/z* 180 (C_1FL) and *m/z* 194 (C_2FL) EICs. Phenanthrene, with three aromatics rings, and its substituted homologues are found at greater second-dimension retention (3.0–3.5 s). The *m/z* 192 (C_1PH) and the *m/z* 206 (C_2PH) EICs show excellent correspondence with the GC × GC peak patterns. Interleaved with the phenanthrene peaks are dibenzothiophene peaks. Again, the volatility and polarity similarities of the two groups lead to similar placement in the GC × GC chromatogram given the stationary phases chosen for the two dimensions in this experiment. The *m/z* 198 (C_1DBT) and *m/z* 212 (C_2DBT) EICs show excellent correspondence with the GC × GC peak patterns. In Figure 3, only the identity of phenanthrene (PH) and dibenzothiophene (DBT) are definitively known by using chemical standards. However, by using the EICs and chemical logic based on volatility and polarity information, the identity of other peaks and classification of the other bands is straightforward. Peaks numbered on the EICs in Figure 3 are identified in Table 3.

A GC × GC chromatogram region containing carbon substituted chrysenes (C_1CH, C_2CH), and substituted benzo-

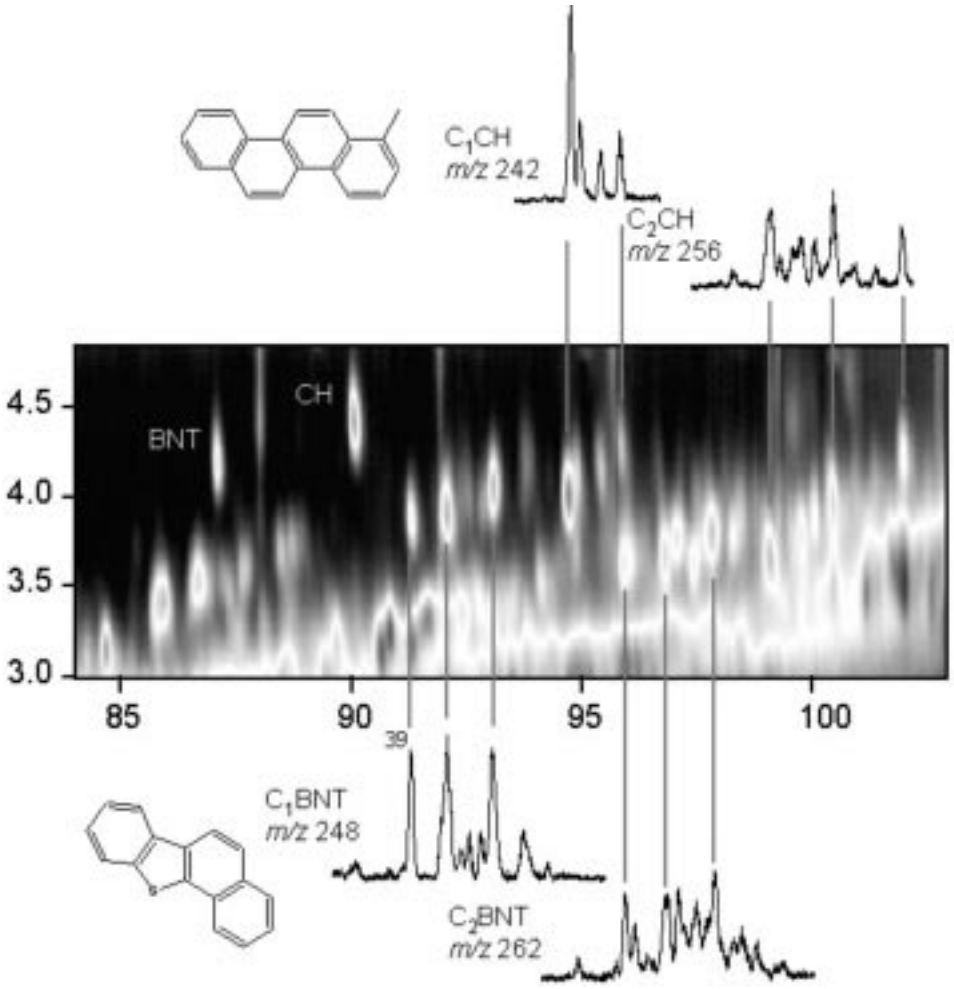

Figure 4. Extracted region of the GC × GC chromatogram. Benzo[*b*]naphtho[2,1-*d*]thiophene (BNT) and chrysene (CH) peaks are identified. GC/MS extracted ion chromatograms (EIC) of substituted benzonaphthothiophenes (C_xBNT) and chrysenes (C_xCH) are overlaid for identification and comparison. Peaks numbered on each EIC are identified in Table 3. The structures of 1-methylchrysene and benzo[*b*]naphtho[2,1-*d*]thiophene are included for reference.

naphthothiophenes (C_1BNT, C_2BNT) is shown in **Figure 4**. The interleaving of these groups of peaks is almost identical to that observed for the phenanthrenes and dibenzothiophenes in Figure 3. The only difference is that chrysene has one more aromatic ring than phenanthrene, and benzonaphthothiophene has one more aromatic ring than dibenzothiophene, so the pattern is shifted six-carbons to the right in the GC × GC chromatogram. The additional aromatic ring produces even more second-dimension retention (3.5–4.5 s) for these bands. Here again, the corresponding *m/z* 242, 256, 248, and 262 EICs, chemical logic, and the repeating patterns in the GC × GC chromatogram provide support for the peak identifications. Peaks numbered on each EIC in Figure 4 are identified in Table 3.

Figure 5 shows a GC × GC chromatogram of the sterane, hopane, and triaromatic sterane biomarker groups. These biomarkers are frequently used to monitor the biodegradation of spilled oil and to calculate maturity parameters used in petroleum exploration. Modifications to the thermal modulator instrumentation, specifically the use of an independent temperature zone for the modulator tube, have extended the volatility range of the GC × GC analysis to C_{40} *n*-alkanes. This allows the GC × GC separation and identification of these important biomarker classes. The sterane band is the group of numerous peaks from about 100 to 115 min on the first dimension and about 1.0 s on the second dimension. The tetracyclic structure of the steranes contributes to the polarity of the molecule and results in more second-dimension retention than the

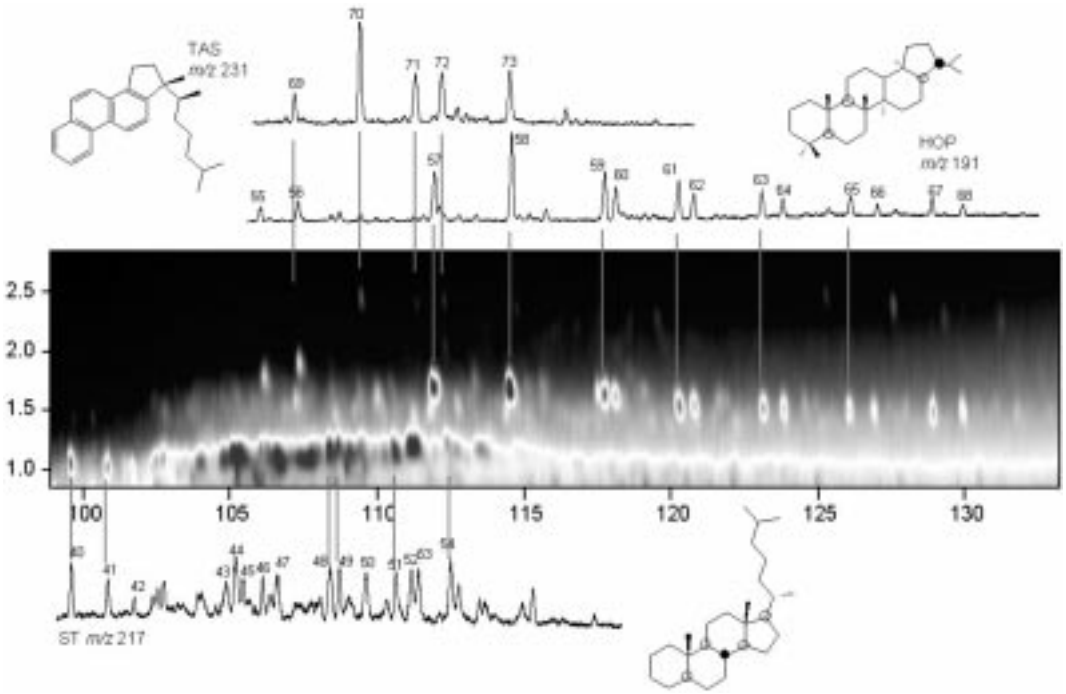

Figure 5. Extracted region of the GC × GC chromatogram. GC/MS extracted ion chromatograms (EIC) of triaromatic steranes (TAS), hopanes (HOP), and steranes (ST) are overlaid for identification and comparison. Peaks numbered on each EIC are identified in Table 3. The structures of 5α,14α,17α(*H*)-cholestane (20*R*) (peak 46), 17α,21β(*H*)-hopane (peak 58) and cholestane (20S) (peak 69) are included for reference [6].

alkane and branched alkane components in crude oil. Each sterane component has the *m/z* 217 fragment in its mass spectrum so the *m/z* 217 EIC has many peaks in common with the GC × GC peak pattern. The hopane band is the prominent band of peaks spanning the GC × GC chromatogram at approximately 1.5 s retention on the second dimension. Hopanes are slightly more polar than steranes, (pentacyclic vs. tetracyclic), so they have more second-dimension retention. Each hopane biomarker has the *m/z* 191 fragment in its mass spectrum. Therefore, the *m/z* 191 EIC has good peak-to-peak correspondence with the peak pattern in the GC × GC chromatogram. Tricyclic and tetracyclic triterpanes also have *m/z* 191 mass fragments, but only the portion of the *m/z* 191 EIC containing the pentacyclic hopanes is shown in the figure. The location of the tricyclic and tetracyclic triterpanes in the GC × GC chromatogram has not yet been determined. The trace components peaks from about 105 to 120 min on the first dimension and at the top of the chromatogram (2.5 s retention) are triaromatic steranes. The greater second-dimension retention is expected because of the aromatic rings in these components. Since triaromatic steranes have a common mass spectrum fragment at *m/z* 231, that EIC corresponds to the GC × GC peak pattern. In Figure 5, each of the EICs represents molecule fragments rather than molecular ions. One effect is that some of the EICs have peaks that do not directly correspond to peaks in a single GC × GC band. For example, in the *m/z* 191 EIC there are a few small peaks between 125 and 130 min that may correspond better with a GC × GC band at 2.5 s second-dimension retention than the identified hopane band at 1.5 s retention. This suggests that there are petroleum components that produce a *m/z* 191 fragment but that are not hopanes. Further investigation of these peak patterns is underway.

4 Conclusion

Petroleum biomarker components were separated from crude oil and their peak patterns were interpreted in the GC × GC chromatogram image. The GC × GC biomarker peak patterns showed excellent correspondence to GC/MS extracted ion chromatograms. The correspondence exists because both methods are two-dimensional. Both employ a volatility-based separation on the first dimension, but GC/MS in EIC mode uses a mass-filter on the second dimension while GC × GC uses a polarity-based separation mechanism on the second dimension. Differences appear when GC/MS EICs include components with a common mass fragment that are otherwise structurally and chemically unrelated. The GC × GC chromato-

gram on the other hand only groups components by structural and chemical similarities. One advantage of the GC × GC image over GC/MS EICs is that all biomarker bands are simultaneously visible in the GC × GC image and that unknown petroleum components or minor differences between petroleum samples are easily observable. Visual identification of biomarkers followed by component peak integration makes GC × GC a valuable tool for forensic petroleum identification and petroleum geochemistry investigations. A more advanced tool for biomarker identification is a GC × GC separation coupled with MS detection. The GC × GC/MS combination can produce full-scan, interpretable mass spectra of the petroleum biomarker components [15, 16]. This information can help decode more complex peak patterns in the GC × GC chromatogram.

Acknowledgments

The Robert T. Alexander Trust provided partial funding for this work. Mention of trade names in the article does not indicate U.S. Coast Guard endorsement of any kind. This article has not been subject to official review and no endorsement should be inferred.

References

[1] G. Eglinton, M. Calvin, *Scientific American*, **1967**, *216*, 32.

[2] J.K. Volkman, A.T. Revill, A.P. Murray, in: R.P. Eganhouse (ed), *ACS Symposium Series 671, Molecular Markers in Environmental Geochemistry*, American Chemical Society, Washington, DC 1997, chapter 8.

[3] K.E. Peters, J.M. Moldowan, *The Biomarker Guide. Interpreting Molecular Fossils in Petroleum and Ancient Sediments*, Prentice Hall, New Jersey 1993.

[4] P.D. Boehm, G.S. Douglas, W.A. Burns, P.J. Mankiewicz, D.S. Page, A.E. Bence, *Mar. Pollut. Bull.* **1997**, *34*, 599.

[5] Z. Wang, M. Fingas, D.S. Page, *J. Chrom. A*. **1999**, *843*, 369.

[6] D.W. Waples, T. Machihara, *Biomarkers for Geologists – A Practical Guide to the Application of Steranes and Triterpanes in Petroleum Geology*, AAPG Methods in Exploration, No. 9, The American Association of Petroleum Geologists, Tulsa, OK 1991.

[7] J.B. Phillips, J. Beens, *J. Chrom. A*. **1999**, *856*, 331.

[8] W. Bertsch, *J. High Resol. Chromatogr.* **2000**, *23*, 167.

[9] G.S. Frysinger, R.B. Gaines, *J. High Resol. Chromatogr.* **2000**, *23*, 197.

[10] G.S. Frysinger, R.B. Gaines, E.B. Ledford, *J. High Resol. Chromatogr.* **1999**, *22*, 195.

[11] J.B. Phillips, C.J. Venkatramani, *J. Microcol. Sep.* **1993**, *5*, 511.

[12] J. Blomberg, P.J. Schoenmakers, J. Beens, R. Tijssen, *J. High Resol. Chromatogr.* **1997**, *20*, 539.

[13] J. Beens, H. Boelens, R. Tijssen, J. Blomberg, *J. High Resol. Chromatogr.* **1998**, *21*, 47.

[14] R.B. Gaines, G.S. Frysinger, M.S. Hendrick-Smith, J.D. Stuart, *Environ. Sci. & Technol.* **1999**, *33*, 2106.

[15] G.S. Frysinger, R.B. Gaines, *J. High Resol. Chromatogr.* **1999**, *22*, 251.

[16] M. van Deursen, J. Beens, J. Reijenga, P. Lipman, C. Cramers, J. Blomberg, *J. High Resol. Chromatogr.* **2000**, *23*, 507.

[17] J.B. Phillips, R.B. Gaines, J. Blomberg, P. Schoenmakers, F.W.M. van der Wielen, J.-M. Dimandja, V. Green, J. Granger, D. Patterson, L. Racovalis, H.-J. de Geus, J. de Boer, P. Haglund, J. Lipsky, E.B. Ledford, *J. High Resol. Chromatogr.* **1999**, *22*, 1.

[18] A.E. Bence, K.A. Kvenvolden, M.C. Kennicut II, *Org. Geochem.* **1996**, *24*, 7.

[19] K.A. Kvenvolden, F.D. Hostettler, P.R. Carlson, J.B. Rapp, C.N. Threlkeld, A.Warden, *Environ. Sci. Technol.* **1995**, *29*, 2684.

[20] P.D. Boehm, D.S. Page, E.S. Gilfillan, A.E. Bence, W.A. Burns, P.J. Mankiewicz, *Environ. Sci. Technol.* **1998**, *32*, 567.

[21] H. Budzinski, N. Raymond, T. Nadalig, M. Gilewicz, P. Garrigues, J.C. Bertrand, P. Caumette, *Org. Geochem.* **1998**, *28*, 337.

[22] B.G.K. van Aarssen, T.P. Bastow, R. Alexander, R.I. Kagi, *Org. Geochem.* **1999**, *30,* 1213.

[23] R. Trolio, K. Grice, S.J. Fisher, R. Alexander, R.I. Kagi, *Org. Geochem.* **1999**, *30,* 1241.

[24] A. Chakhmakhchev, M. Suzuki, K. Takayama, *Org. Geochem.* **1997**, *26,* 483.

[25] Z. Wang, M. Fingas, *Environ. Sci. Technol.* **1995**, *29*, 2842.

[26] S.G. Mossner, M.J. Lopez de Alda, L.C. Sander, M.L. Lee, S.A. Wise, *J. Chrom. A*. **1999**, *841*, 207.

[27] S.G. Mossner, S.A. Wise, *Anal. Chem.* **1999**, *71*, 58.

[28] D.L. Vassilaros, R.C. Kong, D.W. Later, M.L. Lee, *J. Chrom.* **1982**, *252*, 1.

[29] D. Munoz, P. Doumenq, M. Guiliano, F. Jacquot, P. Scherrer, G. Mille, *Talanta*, **1997**, *45*, 1.

[30] A.O. Barakat, A.R. Mostafa, J. Rullkotter, A. Rahman Hegazi, *Mar. Pollut. Bull.* **1999**, *38*, 535.

[31] K.M. Rogers, J.D. Collen, J.H. Johnston, N.E. Elgar, *Org. Geochem.* **1999**, *30,* 593.

[32] Z. Wang, M. Fingas, *LCGC*, **1995**, *13*, 950.

[33] Z. Wang, M. Fingas, G. Sergy, *Environ. Sci. Technol.* **1994**, *28*, 1733.

[34] A.O. Barakat, *J. High Resol. Chromatogr.* **1994**, *17*, 549.